NANOSYSTEMS:
PHYSICS, CHEMISTRY, MATHEMATICS

Original article

Lomakin M.S. *Nanosystems: Phys. Chem. Math.*, 2025, **16** (2), 235–242.
http://nanojournal.ifmo.ru
DOI 10.17586/2220-8054-2025-16-2-235-242

Phase formation in the Na_2O–Bi_2O_3–Fe_2O_3–MoO_3–(H_2O) system

Makariy S. Lomakin[1,2,a]

[1]Ioffe Institute, St. Petersburg, Russia

[2]Branch of Petersburg Nuclear Physics Institute named by B.P. Konstantinov of National Research Centre "Kurchatov Institute" – Institute of Silicate Chemistry, St. Petersburg, Russia

[a]lomakinmakariy@gmail.com

ABSTRACT The effect of the hydrothermal fluid pH on the chemical and phase composition, as well as the size parameters and morphology of crystallites and particles of hydrothermal synthesis products formed in the Na_2O–Bi_2O_3–Fe_2O_3–MoO_3 system at $T = 170$ °C and $P < 7$ MPa has been studied. It has been established that in the acidic pH region, the bulk chemical composition of the hydrothermal synthesis products is depleted relative to the nominal composition specified for the synthesis in iron oxide, while in the alkaline pH region, it is depleted in molybdenum oxide and, to a lesser extent, in bismuth oxide, while the best correspondence between the nominal and bulk composition observed at pH = 2. It is shown that in the pH range from 2 to 6 new compounds of variable composition ($Na_{0.19-0.47}Bi_{0.42-0.85}Fe_{0.14-0.31}MoO_y$) with a scheelite-like structure (sp. gr. $I\bar{4}$, No. 82) are formed, which have not been previously described in the scientific literature. These compounds with the smallest mean crystallite size (∼25 nm) were obtained at pH = 2, and it was shown that under these conditions polycrystalline plate-like particles (thickness (h) ∼50–150 nm) are formed, often having a curved shape, which grow together to form agglomerates with a "flower-like" morphology. It was found that fluorite-type solid solutions ($Bi_{3.65-4.30}Fe_{0.37-0.45}MoO_z$) are formed in alkaline media (isostructured to the oxide δ-Bi_2O_3 (sp. gr. $Fm\bar{3}m$, No. 225)).

KEYWORDS hydrothermal synthesis, sodium bismuth iron molybdate, scheelite-like structure, nanocrystals, fluorite-type solid solutions.

ACKNOWLEDGEMENTS XRD, SEM and EDXMA studies were performed employing the equipment of the Engineering Center of the St. Petersburg State Institute of Technology (Technical University). The author expresses his deep gratitude to Corr. Mem. RAS Victor Vladimirovich Gusarov for valuable comments and advice on improving the quality of the manuscript. The work was financially supported by the Russian Science Foundation (Project No. 24-13-00445).

FOR CITATION Lomakin M.S. Phase formation in the Na_2O–Bi_2O_3–Fe_2O_3–MoO_3–(H_2O) system. *Nanosystems: Phys. Chem. Math.*, 2025, **16** (2), 235–242.

1. Introduction

Multicomponent molybdates are the objects of active research, since representatives of this class of complex oxides have a wide range of physicochemical properties that are interesting for study [1]. Bismuth molybdate, Bi_2MoO_6, is a single-layer Aurivillius phase consisting of $[Bi_2O_2]^{2+}$ layers sandwiched between $[MoO_4]^{2-}$ slabs and could be used as potential LIB anode material [2, 3] and outstanding photocatalyst [4]. Bismuth iron molybdate, $Bi_3(FeO_4)(MoO_4)_2$, has a monoclinic structure related to the scheelite ($CaWO_4$) structure and could be used as a good photocatalyst for water splitting and photodegradation of organic contamination [5, 6]. Sodium bismuth molybdate, $NaBi(MoO_4)_2$, as well as other related compounds of $M^IM^{III}(MoO_4)_2$ stoichiometry, has a tetragonal scheelite-like structure and could be potentially used as host crystals for active ions having luminescence properties [7–9].

Obtaining the mentioned compounds, as well as other multicomponent molybdates, using low-temperature synthesis methods in aqueous environments, including hydrothermal conditions, can ensure their formation in nanocrystalline form, which can potentially lead to the discovery of new unique properties [10]. In addition, lowering the synthesis temperature may lead to the discovery of new compounds that are unstable at elevated temperatures [11]. For example, in the Bi_2O_3–Fe_2O_3–WO_3 system, the formation of new compounds of variable composition with a cubic pyrochlore structure under hydrothermal conditions (T = 90 – 200 °C, $P \leq$7 MPa) was established, the upper temperature limit of stability of which is ∼ 725 °C [12, 13].

The relevance of the work is related to the study of phase formation in the previously unexplored Na_2O–Bi_2O_3–Fe_2O_3–MoO_3–(H_2O) system and the accumulation of information that can provide a basis for obtaining new multicomponent molybdates, including in the form of nanoparticles and nanocomposites with unique properties. The aim of the work is to study the influence of the hydrothermal fluid pH on the chemical and phase composition, as well as the size parameters and morphology of crystallites and particles of hydrothermal synthesis products formed in the Na_2O–Bi_2O_3–Fe_2O_3–MoO_3 system.

© Lomakin M.S., 2025

2. Materials and Methods

2.1. Synthesis section

The synthesis procedure, which is the same for all samples, is described below. Nominal composition specified for the synthesis corresponded to the following atomic ratios: (1) $Bi_{0.50}Fe_{0.37}MoO_{4.31}$ and (2) $Bi_{0.84}Fe_{0.56}MoO_{5.10}$. To obtain a sample, 2 mmol of crystalline hydrate of bismuth (III) nitrate, $Bi(NO_3)_3{\cdot}5H_2O$ (puriss. spec.), and (1) 1.48 or (2) 1.33 mmol of crystalline hydrate of iron (III) nitrate, $Fe(NO_3)_3{\cdot}9H_2O$ (pur.), were dissolved in 5 ml of 6 M HNO_3 (puriss. spec.), after which 25 ml of distilled water was added to the resulting solution. Next, (1) 4 or (2) 2.38 mmol of sodium molybdate (VI) crystalline hydrate, $Na_2MoO_4{\cdot}2H_2O$ (puriss. spec.), was dissolved in 20 ml of distilled water and the resulting solution was added dropwise into the acidic solution of bismuth and iron nitrates stirred with a magnetic stirrer at 800 rpm ($\sim$30 mL of distilled water was then added there and used to rinse the beaker that had contained the sodium molybdate solution). After stirring the obtained suspension for 1 h, a solution of 2 M NaOH was added to it dropwise until reaching pH of a certain value (1 (no NaOH), 2, 4, 6, 8, 10). The amorphous precursor suspension obtained this way, was additionally stirred at 1000 rpm for $\sim$1 h and then transferred into Teflon chambers ($\sim$80% filling) and placed in steel autoclaves, which were then put in a furnace heated up to T = 170 °C. After 66 h, the autoclaves were removed from the furnace and cooled in air. The resulting precipitates were separated from the mother liquor (it was poured out), rinsed with distilled water several times by decantation and dried at 90 °C for 24 h.

2.2. Characterization

The crystal structure of the synthesized samples was analyzed by XRD using an X-ray powder diffractometer DRON-8N (IC "Burevestnik", Russia) in the Bragg-Brentano geometry (an X-ray tube with copper anode, Ni K_β filter, Cu-K_α radiation (average wavelength λ = 1.54186 Å)), equipped with a position-sensitive (PSD) linear detector Mythen2 R 1D (DECTRIS Ltd., Switzerland) with an opening angle of 4.48° and with a single parabolically bent Göbel Mirror placed after the X-ray tube at the primary beam focus. The measurements were carried out in the range of angles $2\theta = 10^\circ - 65^\circ$ with a step of $\Delta 2\theta = 0.0142^\circ$, and the total time at the point was 8 seconds.

X-ray phase analysis of the measured XRD patterns of samples was carried out using the Crystallographica Search-Match program, version 3.1.0.2 (Oxford Cryosystems Ltd., England) using the Powder Diffraction File-2 (PDF-2) [14].

Scanning electron microscopy (SEM) images and bulk elemental composition of the samples, as well as elemental composition of particles belonging to the different morphological motifs (local analysis), were obtained on a Tescan Vega 3 SBH scanning electron microscope (Tescan Orsay Holding, Czech Republic) with an Oxford Instruments Energy Dispersive X-ray Microanalysis (EDXMA) attachment. The relative number of elements was calculated using the AZtec software. When determining the bulk composition the emission spectra were accumulated from three sites of each sample with a total area of $\sim$7 mm^2 and a set of statistics for at least 1 million pulses at each site, then the data were averaged.

3. Results and discussions

3.1. Chemical composition

Nominal composition specified for the synthesis and the EDXMA data on the bulk chemical composition of the samples are presented in Table 1 in the form of atomic ratios. It should be noted that for the two nominal compositions studied ($Bi_{0.50}Fe_{0.37}MoO_{4.31}$ and $Bi_{0.84}Fe_{0.56}MoO_{5.10}$), a similar tendency is observed in the change in the corresponding bulk compositions with a change in the hydrothermal fluid pH. According to the presented data, the best agreement between the nominal and bulk composition is observed for the samples obtained at pH = 2, while for all other samples a noticeable depletion of the bulk composition relative to the nominal one in one or two components is clearly observed: pH = 1 and 4 in Fe_2O_3; pH = 6 in MoO_3; pH = 8 and 10 in Bi_2O_3 and MoO_3. Thus, the observed tendency in the change in the bulk composition relative to the nominal one with a change in the hydrothermal fluid pH resembles that established earlier in the study of the Bi_2O_3–Fe_2O_3–WO_3 system [15]: in the acidic pH region, a depletion of the bulk chemical composition in iron oxide is observed, while in the alkaline pH region, a depletion of the bulk chemical composition in molybdenum oxide and, to a lesser extent, in bismuth oxide is observed; at pH = 2 (at pH =2–5 in [15]), the change in the bulk composition relative to the nominal one is not as significant as at other pH values.

The change in the bulk chemical composition relative to the nominal one is due to the different solubility of the components of the amorphous precursor at different hydrothermal fluid pH values, which leads to their redistribution between the dispersed phase and the dispersion medium of the amorphous precursor suspension subjected to hydrothermal treatment. For this reason, some components may remain dissolved in the cooled mother liquor and will be removed from the system during further rinsing of the sediment.

It is important to note that in the samples obtained at pH = 2, 4 and 6, a noticeable amount of sodium is detected, while in other samples it is absent even in trace amounts.

TABLE 1. Bulk chemical composition of samples synthesized by the hydrothermal method, in rel. at. units, according to the EDXMA data

Sample			Bi/Mo		Fe/Mo		Bi/Fe		Na/Mo	
			Nom.[a]	Bulk	Nom.[a]	Bulk	Nom.[a]	Bulk	Nom.[b]	Bulk
$Bi_{0.50}Fe_{0.37}MoO_{4.31}$	pH	1	0.50	0.55	0.37	0.14	1.35	3.93	–	–
		2		0.53		0.29		1.83		0.26
		4		0.55		0.15		3.67		0.38
		6		1.05		0.36		2.92		0.23
		8		3.09		2.79		1.11		–
		10		4.67		4.59		1.02		–
$Bi_{0.84}Fe_{0.56}MoO_{5.10}$	pH	1	0.84	0.92	0.56	0.37	1.50	2.49	–	–
		2		0.75		0.54		1.39		0.24
		4		0.78		0.38		2.05		0.24
		6		1.08		0.48		2.25		0.22
		8		3.39		3.05		1.11		–
		10		4.32		4.73		0.91		–

[a]Nominal composition specified for the synthesis. [b]Not specified for the synthesis.

The relative error for the Bi/Mo, Fe/Mo, Bi/Fe, and Na/Mo ratios does not exceed 7, 4, 6, and 8 %, respectively.

3.2. XRD analysis

Powder XRD patterns of samples synthesized by the hydrothermal method are shown in Fig. 1 (nominal composition – $Bi_{0.50}Fe_{0.37}MoO_{4.31}$) and Fig. 2 (nominal composition – $Bi_{0.84}Fe_{0.56}MoO_{5.10}$). The change in the bulk chemical composition of samples obtained at different hydrothermal fluid pH values, which was discussed in Section 3.1, leads to a change in their phase composition. The phase composition analysis of the samples, the results of which are presented below, was performed taking into account the data obtained using SEM and local EDXMA (for details see Section 3.3).

In the XRD patterns of the samples obtained at pH = 2 (nominal composition – $Bi_{0.84}Fe_{0.56}MoO_{5.10}$) and 4, reflections of only one phase are observed – $NaBi(MoO_4)_2$ (PDF-2 No. 88-242), which crystallizes in the tetragonal syngony and has a scheelite-like structure (sp. gr. $I\bar{4}$, No. 82). However, the bulk composition of these samples contains a noticeable amount of iron, which, apparently, cannot be attributed to the composition of the amorphous phase, since it is not observed in the samples, due to the absence of signs of an amorphous halo in the XRD patterns. Taking into account the data presented in Section 3.3, it can be concluded that these samples contain only a crystalline phase of variable composition, which is a four-component complex oxide (sodium bismuth iron molybdate) with a scheelite-like structure, apparently, not previously described in the scientific literature. It can be assumed that in the structure of these compounds, the Fe^{3+} cations are located in the same octahedrally coordinated positions as the Mo^{6+} cations, however, a detailed description of the crystal structure of the compounds obtained for the first time will be the subject of further research on this topic. It should be noted that the unit cell parameters (UCP) of the indicated compounds change with a change in their composition, and, apparently, the key factor influencing this is the amount of "large" Bi^{3+} cations, the increase of which is accompanied by an increase in UCP. The calculation of the mean crystallite sizes of the indicated compounds using the Scherrer formula was performed only for single-phase samples obtained at pH = 2 (nominal composition – $Bi_{0.84}Fe_{0.56}MoO_{5.10}$) and 4, since for other samples a superposition of the reflections of the scheelite-like phase with the reflections of the phases coexisting with it was observed. The mean crystallite sizes of the scheelite-like phase, calculated using the Scherrer formula, were: ∼25 nm – pH = 2 (nominal composition – $Bi_{0.84}Fe_{0.56}MoO_{5.10}$); ∼31 nm – pH = 4 (nominal composition – $Bi_{0.84}Fe_{0.56}MoO_{5.10}$); ∼51 nm – pH = 4 (nominal composition – $Bi_{0.50}Fe_{0.37}MoO_{4.31}$).

In addition to the reflections of the above-described scheelite-like phase, the XRD pattern of the sample obtained at pH = 2 (nominal composition – $Bi_{0.50}Fe_{0.37}MoO_{4.31}$) contains reflections of the $Fe_2(MoO_4)_3$ phase (PDF-2 No. 35-183); obtained at pH = 6 (nominal composition – $Bi_{0.50}Fe_{0.37}MoO_{4.31}$) – the Bi_2MoO_6 phase (PDF-2 No. 84-787); obtained at pH = 6 (nominal composition – $Bi_{0.84}Fe_{0.56}MoO_{5.10}$) – the Bi_2MoO_6 (PDF-2 No. 84-787) and $Fe_2(MoO_4)_3$ (PDF-2 No. 35-183) phases. In the XRD patterns of the samples obtained at pH = 1, 8 and 10, reflections of the new scheelite-like phase are not observed, as well as the presence of sodium in the bulk composition of these samples is not detected. This

indicates that only the scheelite-like phase is formed with the participation of sodium, while sodium is not included in the composition of other forming oxide phases, despite the presence of this component in excess in the reaction system.

In the XRD patterns of the samples obtained at pH = 1, reflections of the $Fe_2Mo_3O_{12}$ (PDF-2 No. 80-195), $Bi_2Mo_3O_{12}$ (PDF-2 No. 21-103) and $Bi_3(FeO_4)(MoO_4)_2$ (PDF-2 No. 70-31) phases are observed. The XRD patterns of the samples obtained at pH = 8 and 10 show reflections of a bismuth oxide-enriched phase with the composition $Bi_{3.65-4.30}Fe_{0.37-0.45}MoO_z$ (for details see Section 3.3), which is isostructural to the δ–Bi_2O_3 phase (sp. gr. $Fm\bar{3}m$, No. 225, PDF-2 No. 16-654), and, with the exception of the case of pH = 10 (nominal composition – $Bi_{0.50}Fe_{0.37}MoO_{4.31}$), reflections of other unknown phases are observed, which could not be identified.

It is worth mentioning that the formation in alkaline media of a three-component fluorite-type solid solutions of similar composition, has already been observed in a study of the Bi_2O_3–Fe_2O_3–WO_3 system [15]. However, it is important to note that the obtained samples do not contain a phase with a pyrochlore structure, the formation of which was previously observed in the Bi_2O_3–Fe_2O_3–WO_3 and Na_2O–Bi_2O_3–Fe_2O_3–WO_3 systems [12, 13], despite the use of a similar synthesis procedure and despite a similar electronic structure of the Mo^{6+} and W^{6+} cations.

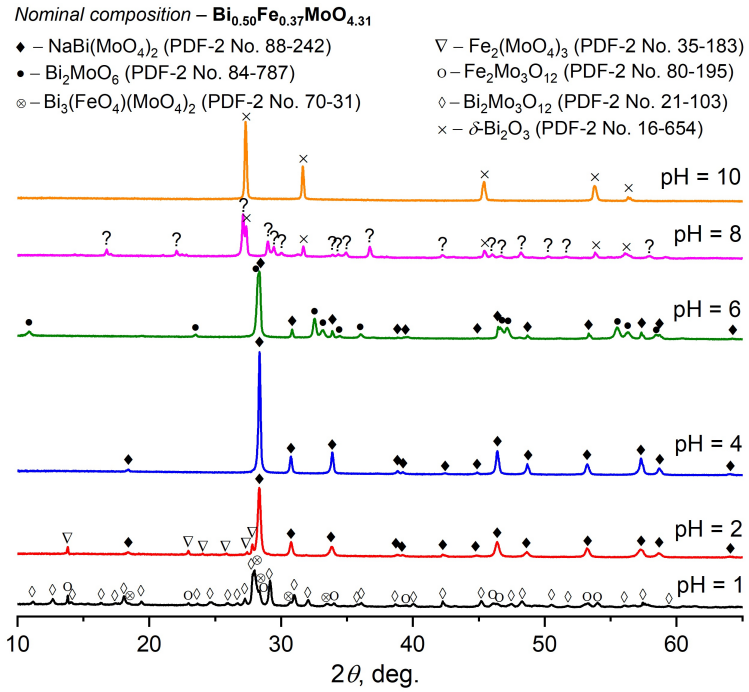

FIG. 1. Powder XRD patterns of samples synthesized by the hydrothermal method (nominal composition – $Bi_{0.50}Fe_{0.37}MoO_{4.31}$)

3.3. SEM

The SEM data for the samples synthesized by the hydrothermal method are shown in Fig. 3 and Fig. 4. In the sample obtained at pH = 2 (nominal composition – $Bi_{0.84}Fe_{0.56}MoO_{5.10}$) (Fig. 3b), large agglomerates (∼5 – 20 μm) are observed, the shape of which is close to spherical, composed of grown together plate-like particles (thickness (h) ∼50 – 150 nm), often having a curved shape. In the voids between the plate-like particles, smaller particles can be found, which makes it practically impossible to identify the composition of particles of different morphological motifs (plate-like and smaller particles) using local EDXMA. In the sample obtained at pH = 4 (nominal composition – $Bi_{0.84}Fe_{0.56}MoO_{5.10}$) (Fig. 3d), particles of two morphological motifs are observed: (1) conditionally spherical particles (∼0.5 – 1.5 μm) and (2) rod-shaped particles (h ∼1 μm and length (l) ∼ 10 μm), as well as agglomerates of these particles (1 and 2). In the back-scattered electron (BSE) detection mode, it can be observed that the particles of the two morphological motifs have the same brightness, which indicates a fairly uniform distribution of different type atoms throughout the sample volume. In addition, local EDXMA data show that the spherical particles have the composition $Na_{0.19}Bi_{0.81}Fe_{0.31}MoO_{4.78}$, while the rod-shaped particles – $Na_{0.30}Bi_{0.85}Fe_{0.22}MoO_{4.76}$, and these atomic ratios are close to the bulk chemical composition of this sample. In the sample obtained at pH = 4 (nominal composition – $Bi_{0.50}Fe_{0.37}MoO_{4.31}$) (Fig. 3c), one can also observe particles of two morphological motifs: (3) conventionally cubic particles (∼2 μm), which are aggregates of smaller particles also having a cubic shape, and (4) aggregates of plate-like particles (h ∼ 150 – 200 nm), grown together with flat sides (“in a stack”). Studies in the BSE mode, as well as local EDXMA data, show that the compositions of particles with different morphologies are similar to each other: cubic particles – $Na_{0.30}Bi_{0.58}Fe_{0.14}MoO_{4.23}$; aggregates

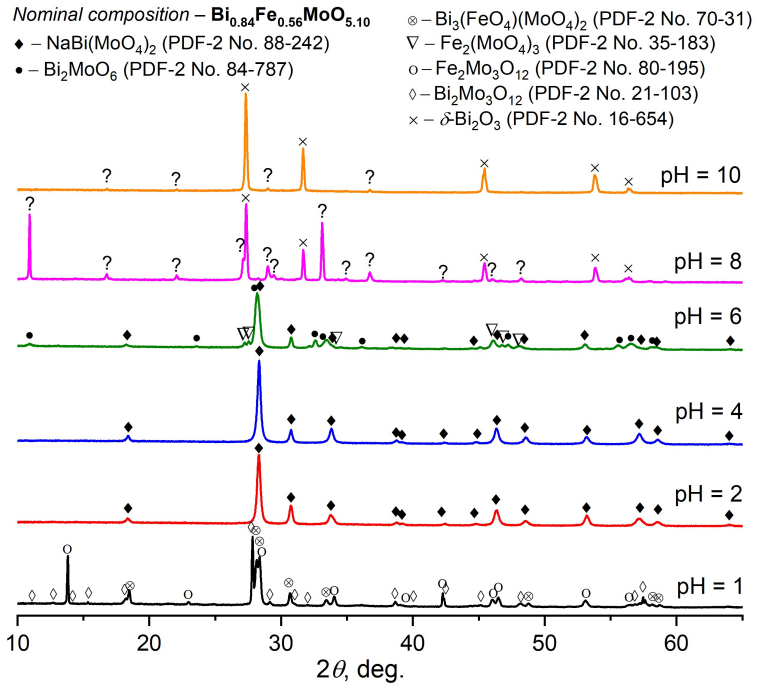

FIG. 2. Powder XRD patterns of samples synthesized by the hydrothermal method (nominal composition – $Bi_{0.84}Fe_{0.56}MoO_{5.10}$)

of plate-like particles – $Na_{0.47}Bi_{0.42}Fe_{0.15}MoO_{4.09}$, and the indicated atomic ratios are close to the bulk chemical composition of this sample. Taking into account the fact that the XRD patterns of the three described samples show reflections of only the scheelite-like phase, it can be concluded that compounds of this structural type were synthesized in the form of particles with different morphology and quantitative chemical composition, which is observed both when comparing different samples with each other, and in each of them. The formation of particles of scheelite-like compounds of two morphological motifs and with slightly different quantitative chemical compositions within a sample could be due to one of the following two reasons. The first reason may be that the reaction system has not reached a state of thermodynamic equilibrium, the achievement of which may be complicated, for example, by the fact that the reacting components are not distributed homogeneously enough throughout the volume of the reaction space, which prevents their direct contact and further interaction. This is a typical problem when using "traditional" methods of mixing the reaction system (magnetic/blade stirrer, etc.), which provide low micro-mixing quality [16]. The second reason may be related to the fact that the reaction system has reached a state of thermodynamic equilibrium, but in this region of chemical compositions at the synthesis temperature and pressure, there is a region of two-phase equilibrium in which two isostructural solid solutions with slightly different quantitative compositions coexist.

The sample obtained at pH = 2 (nominal composition – $Bi_{0.50}Fe_{0.37}MoO_{4.31}$) (Fig. 3a) contains particles of two morphological motifs: (5) large agglomerates of various shapes and sizes, composed of grown together curved plate-like particles (h ~50 – 150 nm), and (6) particles resembling a bar or beam (h ~5 μm and l ~20 – 30 μm), often collected in aggregates of various shapes. In the BSE mode, particles (5) are noticeably lighter than particles (6), while according to the local EDXMA data, particles (5) have the composition $Na_{0.25}Bi_{0.60}Fe_{0.18}MoO_{4.30}$; particles (6) have the composition $Fe_2Mo_3O_{12}$, which is close to the composition of the known compound (PDF-2 No. 35-183).

In the sample obtained at pH = 6 (nominal composition – $Bi_{0.50}Fe_{0.37}MoO_{4.31}$) (Fig. 4a), two morphological motifs are observed: (i) flat plate-like particles (h ~100 nm), growing together at right angles into large, conditionally isometric agglomerates (~2 – 5 μm), and (ii) aggregates of conditionally isometric particles having the shape of a rectangular parallelepiped (h ~0.6 – 0.8 μm) with a square base (~2 – 3 μm). The sample obtained at pH = 6 (nominal composition – $Bi_{0.84}Fe_{0.56}MoO_{5.10}$) (Fig. 4b) also contains particles of two morphological motifs: (i) large particles resembling an elongated spheroid (h ~2 – 3 μm and l ~5 – 10 μm), and (ii) smaller particles "scattered" over these large particles (i), and also forming separate large agglomerates of a conditionally isometric shape (~5 – 10 μm). In these samples (pH = 6), it is practically impossible to identify the composition of particles of different morphological motifs using local EDXMA due to their close contact.

In the sample obtained at pH = 8 (nominal composition – $Bi_{0.50}Fe_{0.37}MoO_{4.31}$) (Fig. 4c), three morphological motifs are observed: (7) octahedral particles (~2 – 4 μm), (8) rod-shaped particles (h ~0.3 – 1 μm and l ~5 – 30 μm) and (9) agglomerates of different sizes without a clearly defined morphology. In the BSE mode, particles (7) and (8)

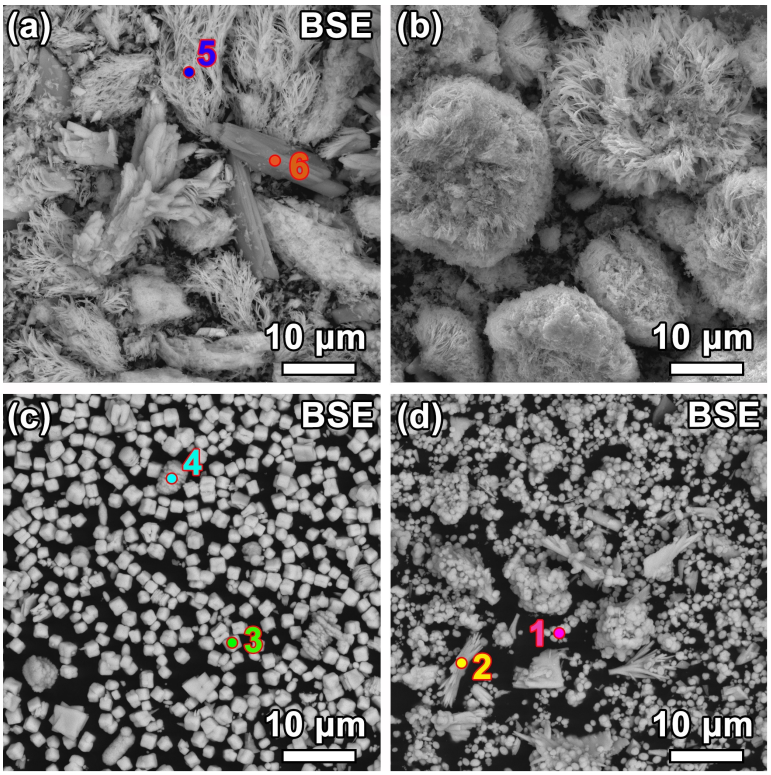

FIG. 3. SEM images of samples synthesized by the hydrothermal method: nominal composition – $Bi_{0.50}Fe_{0.37}MoO_{4.31}$ ((a) pH = 2, (c) pH = 4); nominal composition – $Bi_{0.84}Fe_{0.56}MoO_{5.10}$ ((b) pH = 2, (d) pH = 4)

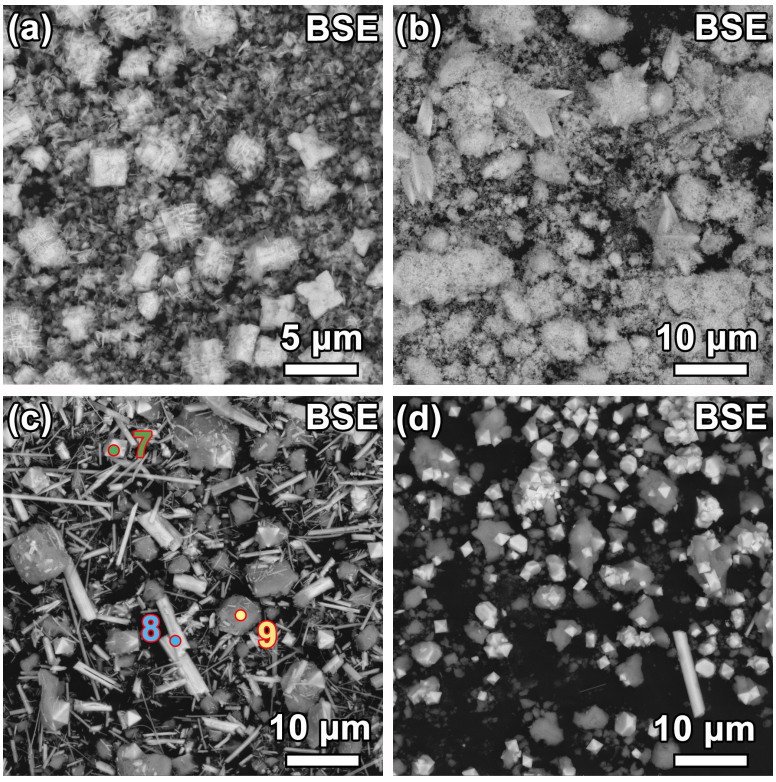

FIG. 4. SEM images of samples synthesized by the hydrothermal method: nominal composition – $Bi_{0.50}Fe_{0.37}MoO_{4.31}$ ((a) pH = 6, (c) pH = 8); nominal composition – $Bi_{0.84}Fe_{0.56}MoO_{5.10}$ ((b) pH = 6, (d) pH = 10)

are noticeably lighter than particles (9), while according to the local EDXMA data, particles (7) have the composition $Bi_{3.65}Fe_{0.45}MoO_{9.15}$; particles (8) – $Bi_{2.76}Fe_{0.31}MoO_{7.61}$; particles (9) – $Bi_{3.67}Fe_{9.45}MoO_{22.68}$. A similar tendency is observed in the case of the sample obtained at pH = 10 (nominal composition – $Bi_{0.84}Fe_{0.56}MoO_{5.10}$) (Fig. 4d), except that the amount of octahedral particles (7) in relation to rod-shaped particles (8) becomes significantly greater. Apparently, the octahedral particles, which have a composition highly enriched in bismuth oxide, are fluorite-type solid solutions that are isostructural to the δ-Bi_2O_3 phase (sp. gr. $Fm\bar{3}m$, No. 225). However, in the crystallographic database PDF-2 it is not possible to find a known compound whose composition would be close to the composition of iron oxide-enriched particles (9), which complicates the phase analysis of these samples.

4. Conclusion

It is shown that the hydrothermal fluid pH has a key effect on the processes of phase formation in the Na_2O–Bi_2O_3–Fe_2O_3–MoO_3 system, determining the chemical and phase composition, as well as the size parameters and morphology of crystallites and particles of hydrothermal synthesis products (T = 170 °C and $P < 7$ MPa).

The discovered tendency in the change in the bulk chemical composition relative to the used nominal compositions ($Bi_{0.50}Fe_{0.37}MoO_{4.31}$ and $Bi_{0.84}Fe_{0.56}MoO_{5.10}$) with a change in the hydrothermal fluid pH resembles that established earlier in the study of the Bi_2O_3–Fe_2O_3–WO_3 system [15]: in the region of acidic pH, a depletion of the bulk chemical composition in iron oxide is observed, while in the region of alkaline pH, a depletion of the bulk chemical composition in molybdenum oxide and, to a lesser extent, in bismuth oxide is observed; at pH = 2 (at pH = 2–5 in [15]), the change in the bulk composition relative to the nominal one is not as significant as at other pH values.

It is shown that in the pH range from 2 to 6 new compounds of variable composition ($Na_{0.19-0.47}Bi_{0.42-0.85}Fe_{0.14-0.31}MoO_y$) with a scheelite-like structure (sp. gr. $I\bar{4}$, No. 82) are formed, which have not been previously described in the scientific literature. The discovered compounds are isostructural with the known compound $NaBi(MoO_4)_2$ (PDF-2 No. 88-242) and, apparently, are formed by isomorphic substitution of some amounts of octahedrally coordinated Mo^{6+} cations by Fe^{3+} cations. It was found that the unit cell parameters (UCP) of these compounds change with a change in their composition, and, apparently, the key influence on this is the number of "large" Bi^{3+} cations, the increase of which is accompanied by an increase in the UCP. An increase in the hydrothermal fluid pH from 2 to 4 leads to an increase in the mean crystallite sizes of the scheelite-like phase, calculated using the Scherrer formula, from ∼25 to ∼30 – 50 nm. The particles of these compounds are polycrystalline, and have different morphology and quantitative chemical composition, which is observed both when comparing different samples with each other, and in each of them. It is shown that the "flower-like" agglomerates of particles formed at pH = 2 have the most developed surface and are grown together plate-like particles (h ∼50 – 150 nm), often having a curved shape, while with an increase in pH, the formation of "denser" aggregates with a significantly smaller number of voids is observed.

It has been shown that fluorite-type solid solutions ($Bi_{3.65-4.30}Fe_{0.37-0.45}MoO_z$) (isostructural with the oxide δ-Bi_2O_3 (sp. gr. $Fm\bar{3}m$, No. 225)) are formed in the region of alkaline pH, the particles of which have a clear octahedral habit, which was previously observed in the study of the Bi_2O_3–Fe_2O_3–WO_3 system [15].

It was established that the obtained samples do not contain a phase with a cubic pyrochlore structure, the formation of which was previously observed in the Bi_2O_3–Fe_2O_3–WO_3 and Bi_2O_3–Na_2O–Fe_2O_3–WO_3 systems [12, 13], despite the use of a similar synthesis procedure and despite a similar electronic structure of the Mo^{6+} and W^{6+} cations.

References

[1] Ray S.K., Hur J. Surface modifications, perspectives, and challenges of scheelite metal molybdate photocatalysts for removal of organic pollutants in wastewater. *Ceramics International*, 2020, **46**, P. 20608–20622.

[2] Yuan S., Zhao Y., Chen W., Wu C., Wang X., Zhang L., Wang Q. Self-assembled 3D hierarchical porous Bi_2MoO_6 microspheres toward high capacity and ultra-long-life anode material for Li-ion batteries. *ACS Appl. Mater. Interfaces*, 2017, **9**, P. 21781–21790.

[3] Zhai X., Gao J., Xue R., Xu X., Wang L., Tian Q. Facile synthesis of Bi_2MoO_6/reduced graphene oxide composites as anode materials towards enhanced lithium storage performance. *J. Colloid Interface Sci.*, 2018, **518**, P. 242–251.

[4] Dai Z., Qin F., Zhao H., Ding J., Liu Y., Chen R. Crystal Defect Engineering of Aurivillius Bi_2MoO_6 by Ce Doping for Increased Reactive Species Production in Photocatalysis. *ACS Catalysis*, 2016, **6**(5), P. 3180–3192.

[5] Nie X., Wulayin W., Song T., Wu M., Qiao X. Surface, optical characteristics and photocatalytic ability of Scheelite-type monoclinic $Bi_3FeMo_2O_{12}$ nanoparticles. *Applied Surface Science*, 2016, **387**, P. 351–357.

[6] Liu B., Yasin A.S., Musho T., Bright J., Tang H., Huang L., Wu N. Visible-Light Bismuth Iron Molybdate Photocatalyst for Artificial Nitrogen Fixation. *Journal of The Electrochemical Society*, 2019, **166**(5), P. H3091–H3096.

[7] Pushpendra, Kunchala R.K., Achary S.N., Tyagi A.K., Naidu B.S. Rapid, Room Temperature Synthesis of Eu^{3+} Doped $NaBi(MoO_4)_2$ Nanomaterials: Structural, Optical, and Photoluminescence Properties. *Cryst. Growth Des.*, 2019, **19**, P. 3379–3388.

[8] Gan Y., Liu W., Zhang W., Li W., Huang Y., Qiu K. Effects of Gd^{3+} codoping on the enhancement of the luminescent properties of a $NaBi(MoO_4)_2$:Eu^{3+} red-emitting phosphors. *J. Alloys Compd.*, 2019, **784**, P. 1003–1010.

[9] Calderón-Olvera R.M., Núñez N.O., González-Mancebo D., Monje-Moreno J.M., Muñoz-Rui M.J., Gómez-González E., Arroyo E., Torres-Herrero B., de la Fuente J.M., Ocaña M. Europium doped-double sodium bismuth molybdate nanoparticles as contrast agents for luminescence bioimaging and X-ray computed tomography. *Inorg. Chem. Front.*, 2023, **10**, P. 3202–3212.

[10] Byrappa K., Adschiri T. Hydrothermal technology for nanotechnology. *Prog. Cryst. Growth Charact. Mater.*, 2007, **53**(2), P. 117–166.

[11] Shandilya M., Rai R., Singh J. Review: hydrothermal technology for smart materials. *Adv. Appl. Ceram.*, 2016, **115**(6), P. 354–376.

[12] Lomakin M.S., Proskurina O.V., Danilovich D.P., Panchuk V.V., Semenov V.G., Gusarov V.V. Hydrothermal Synthesis, Phase Formation and Crystal Chemistry of the pyrochlore/Bi_2WO_6 and pyrochlore/α-Fe_2O_3 Composites in the Bi_2O_3–Fe_2O_3–WO_3 System. *J. Solid State Chem.*, 2020, **282**, P. 121064.

[13] Lomakin M.S., Proskurina O.V., Levin A.A., Nevedomskiy V.N. Pyrochlore phase in the Bi_2O_3–Fe_2O_3–WO_3–(H_2O) system: its stability field in the low-temperature region of the phase diagram and thermal stability. *Nanosyst.: Phys. Chem. Math.*, 2024, **15**(2), P. 240–254.

[14] Fawcett T.G., Kabekkodu S.N., Blanton J.R., Blanton T.N. Chemical analysis by diffraction: the Powder Diffraction File™. *Powder Diffr.*, 2017, **32**, P. 63–71.

[15] Lomakin M.S., Proskurina O.V., Gusarov V.V. Influence of Hydrothermal Synthesis Conditions on the Composition of the Pyrochlore Phase in the Bi_2O_3–Fe_2O_3–WO_3 system. *Nanosyst.: Phys. Chem. Math.*, 2020, **11**(2), P. 246–251.

[16] Lomakin M.S., Proskurina O.V., Abiev R.Sh., Nevedomskiy V.N., Leonov A.A., Voznesenskiy S.S., Gusarov V.V. Pyrochlore Phase in the Bi_2O_3–Fe_2O_3–WO_3–(H_2O) System: Physicochemical and Hydrodynamic Aspects of its Production Using a Microreactor with Intensively Swirled Flows. *Adv. Powder Technol.*, 2023, **34**(7), P. 104053.

Submitted 10 October 2024; accepted 24 November 2024

Information about the authors:

Makariy S. Lomakin – Ioffe Institute, 26, Politekhnicheskaya St., 194021, St. Petersburg, Russia; Branch of Petersburg Nuclear Physics Institute named by B.P. Konstantinov of National Research Centre "Kurchatov Institute" – Institute of Silicate Chemistry, 2, Makarov Emb., 199034, St. Petersburg, Russia; ORCID 0000-0001-5455-4541; lomakin-makariy@gmail.com

Conflict of interest: the authors declare no conflict of interest.